

RESEARCH ARTICLE

Spectral tuning of Amazon parrot feather coloration by psittacofulvin pigments and spongy structures

Jan Tinbergen*, Bodo D. Wilts and Doekele G. Stavenga†

Computational Physics, Zernike Institute for Advanced Materials, University of Groningen, NL-9747 AG Groningen, The Netherlands

*Deceased

†Author for correspondence (d.g.stavenga@rug.nl)

SUMMARY

The feathers of Amazon parrots are brightly coloured. They contain a unique class of pigments, the psittacofulvins, deposited in both barbs and barbules, causing yellow or red coloured feathers. In specific feather areas, spongy nanostructured barb cells exist, reflecting either in the blue or blue-green wavelength range. The blue-green spongy structures are partly enveloped by a blue-absorbing, yellow-colouring pigment acting as a spectral filter, thus yielding a green coloured barb. Applying reflection and transmission spectroscopy, we characterized the Amazons' pigments and spongy structures, and investigated how they contribute to the feather coloration. The reflectance spectra of Amazon feathers are presumably tuned to the sensitivity spectra of the visual photoreceptors.

Supplementary material available online at <http://jeb.biologists.org/cgi/content/full/216/23/4358/DC1>

Key words: barbs, barbules, melanin, thin films, vision.

Received 28 May 2013; Accepted 20 August 2013

INTRODUCTION

Parrots are well known for their striking, bright coloration (Berg and Bennett, 2010). When at rest, most Amazon parrots show a predominantly green colour (Fig. 1), but feathers with bright yellow, red or blue colours are also widespread. The feather colours result from the cumulative reflections from the feather components, the barbs and barbules (Prum, 2006), which in Amazon parrots are often differently coloured. The yellow and red colours are commonly referred to as pigmentary colours, as they are caused by pigments that selectively absorb short-wavelength light. As a consequence, only the long-wavelength part of broad-band incident light remains as back-scattered, reflected light. However, the colour of blue feathers is called a structural colour, because it originates from unpigmented, nano-sized, spongy-structured cells that selectively reflect short-wavelength light by constructive interference (Shawkey et al., 2003; Prum, 2006; Kinoshita et al., 2008; Berg and Bennett, 2010; Stavenga et al., 2011b). The green feathers also have spongy cells, which reflect blue-green light. A blue-absorbing pigment, which functions as a short-wavelength filter, restricts the wavelength range of the reflected light, resulting in green coloured feathers (Berg and Bennett, 2010; D'Alba et al., 2012; Saranathan et al., 2012).

The most common pigments of birds are melanins and carotenoids (McGraw, 2006a; McGraw, 2006b). The melanins are usually incorporated in pigment granules, the melanosomes. Their very broad absorbance spectrum causes a black or brownish pigmentary coloration (McGraw, 2006c). In many bird species, the melanosomes of barbules are arranged in orderly arrays, which then cause structural colorations ranging from violet to purple-red to broad-band whitish (Greenewalt et al., 1960; Durrer, 1977; Osorio and Ham, 2002; Prum, 2006; Stavenga et al., 2011a). However, in parrots, melanosome-based structural colours are unknown.

Instead of the carotenoids, parrot feathers contain a special class of pigment, called the psittacofulvins, after the family name, the psittacines or Psittaciformes (McGraw and Nogare, 2004; McGraw and Nogare, 2005; McGraw, 2006b; Berg and Bennett, 2010). Both the carotenoids and psittacofulvins have rather narrow-band absorbance spectra, with absorption bands restricted to the violet, blue or blue-green wavelengths, yielding (pale-)yellow or red pigmentary colours. The carotenoids and psittacofulvins are easily confused in spectral measurements, but detailed chemical and Raman spectroscopical research has clearly documented their differences (Veronelli et al., 1995; Stradi et al., 2001). The psittacofulvins are probably enzymatically derived from carotenoids (McGraw and Nogare, 2004; McGraw, 2006b), but the parrot pigments seem to be an independent evolutionary development (Stoddard and Prum, 2011). Why this has occurred, that is, what special benefit is provided by the psittacofulvins, is somewhat enigmatic.

To gain insight into these questions we have performed a quantitative study of the different coloration techniques employed by the Amazon parrots. We measured the absorbance spectra and density of various psittacofulvins and investigated how they are combined with melanin pigmentation as well as with different spongy structures that together produce the Amazons' colourful plumage. We furthermore compared the feather coloration, i.e. the feather reflectance, with the spectral sensitivity of the birds' visual photoreceptors.

MATERIALS AND METHODS

Amazon parrot feathers

We obtained feathers of various Amazon parrots [Natterer's Amazon, *Amazona ochrocephala nattereri* (Finsch 1865); Panama yellow-headed Amazon, *Amazona ochrocephala panamensis*



Fig. 1. A Panama Amazon parrot, *Amazona ochrocephala panamensis*.

(Cabanis 1874); and orange-winged Amazon, *Amazona amazonica* (Linnaeus 1766)] from the parrot rescue centre Stichting Papegaaiehulp (Erica, The Netherlands; assistant curator Nathalie van der Vechte).

Spectroscopy

Reflectance spectra of the wings were measured with an Avantes 2048-2 CCD detector array spectrometer using a bifurcated probe (Avantes FCR-7UV200; Avantes, Eerbeek, The Netherlands) or a microspectrophotometer (MSP) constructed from a Leitz Ortholux microscope (see Stavenga et al., 2011b). In the MSP, the microscope objective was an Olympus 20 \times , NA 0.46 (Tokyo, Japan). The light source was a deuterium/halogen [AvaLight-D(H)-S, Avantes, Eerbeek, The Netherlands] or xenon arc lamp (Osram XBO 150W, Munich, Germany). The reference was a diffuse white reflectance tile (Avantes WS-2). The absorbance spectra of the pigments were determined by transmission microspectrophotometry on barbules immersed in refractive index fluids (Cargille Labs, Cedar Grove, NJ, USA).

Anatomy

The anatomical structure of the feather barbs and barbules was studied, after sputtering with palladium, with an XL30-ESEM (Philips, Eindhoven, The Netherlands) scanning electron microscope.

Photoreceptor spectral sensitivities

The eyes of parrots have four classes of single cone photoreceptors, UVS, SWS, MWS and LWS, sensitive in the ultraviolet, blue, green and red wavelength range, respectively (Bowmaker et al., 1997; Hart and Vorobyev, 2005; Berg and Bennett, 2010). Their spectral sensitivities are due to four different visual pigments, filtered by specific oil droplets [transparent (T), clear (C), yellow (Y) and red (R)] positioned in front of the visual-pigment-containing part of the photoreceptor, the outer segment. The C, Y and R droplets contain carotenoids (Goldsmith et al., 1984; Stavenga and Wilts, 2013). The spectral characteristics of the visual pigments have been well studied in the closely related budgerigar, *Melopsittacus undulatus*. We assumed that Amazon parrots have visual pigments with the same peak wavelengths: λ_{\max} =371, 440, 499 and 566 nm, expressed in the UVS, SWS, MWS and LWS photoreceptors, respectively

(Bowmaker et al., 1997). The spectral sensitivities (S) of the cone photoreceptors were calculated using the following equation: $S(\lambda)=T_o(\lambda)T_d(\lambda)\{1-\exp[-d\kappa_{\max}P(\lambda)]\}$, where λ is the wavelength, $T_o(\lambda)$ is the transmittance of the ocular media, $T_d(\lambda)$ is the oil droplet transmittance, d is the cone photoreceptor length, κ_{\max} is the peak absorption coefficient of the visual pigment and $P(\lambda)$ is the normalized visual pigment absorption spectrum. For $T_o(\lambda)$ we used the transmittance spectrum of the ocular lens of a parrot closely related to the Amazons, the crimson rosella, *Platyercus elegans* (Carvalho et al., 2011); this spectrum is very similar to the transmittance spectrum of the ocular media of the starling, *Sturnus vulgaris*, considered to be applicable for the budgerigar (Hart et al., 1998). The transmittance of the transparent oil droplet was assumed to be $T_d(\lambda)=1$, and the other oil droplet transmittances were approximated by $T_d(\lambda)=\exp\{-\exp[-b(\lambda-\lambda_0)]\}$, with values of b and λ_0 for the C-, Y- and R-type oil droplets of $b=0.086$, 0.033 and 0.054, and $\lambda_0=425$, 537 and 587 nm, respectively [table 1 in Hart and Vorobyev (Hart and Vorobyev, 2005)]. We took $d=16\ \mu\text{m}$ and $\kappa_{\max}=0.035\ \mu\text{m}^{-1}$ [equivalent to a decadic absorbance coefficient of $0.014\ \mu\text{m}^{-1}$ (see Hart and Vorobyev, 2005)], and we calculated $P(\lambda)$ using λ_{\max} and a rhodopsin template (Govardovskii et al., 2000).

RESULTS

Pigmentary coloration

As a first example of Amazon feather coloration, Fig. 2A shows a feather of a Natterer's Amazon, which has white, yellow and red parts. The red feather area, observed with incident and transmitted light, reveals the barbs and its branches, the barbules (Fig. 2B,C). Measurement of the feather reflectance with a bifurcated probe

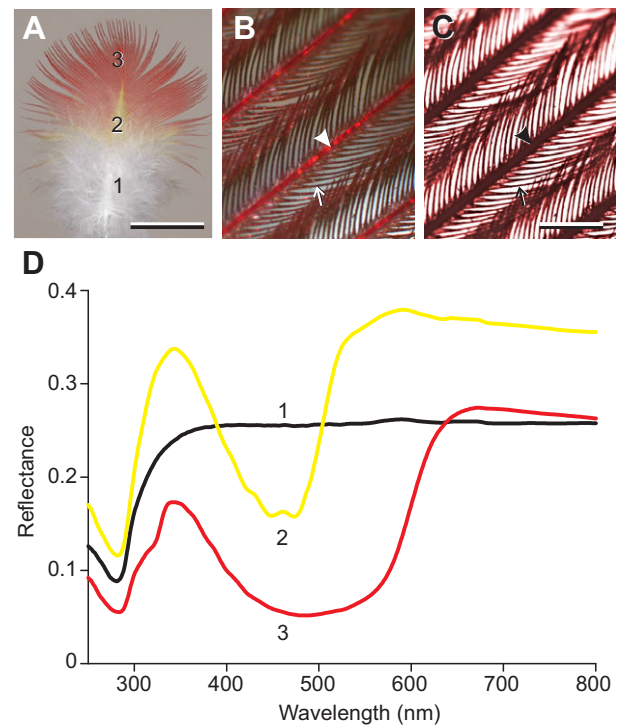


Fig. 2. A feather of a Natterer's Amazon, *Amazona ochrocephala nattereri*, and reflectance spectra. (A) The feather with white (1), yellow (2) and red (3) parts. Scale bar, 1 cm. (B) Detail of the red feather area observed with epi-illumination, showing the red-coloured barbs (arrowhead) and barbules (small arrow). (C) The same area observed with transmitted light. Scale bar (also applies to B), 200 μm . (D) Reflectance spectra of the three areas shown in A, measured with a bifurcated probe.

yielded for the white area an approximately flat spectrum in the visible wavelength range, with a distinct trough at ~ 280 nm (Fig. 2D, curve 1). The trough is also seen in the reflectance spectra of the yellow and red feather areas (Fig. 2D, curves 2 and 3), as well as in spectra of white feathers of other birds (not shown): the trough is due to absorption by keratin. The spectra of the yellow and red feather areas have additional valleys around 450 and 500 nm, indicating the presence of two different pigments, absorbing in the blue and blue-green wavelength ranges, respectively. The latter reflectance spectra differ in height at wavelengths >650 nm, because of differences in the packing density of the barbules; the slight decrease in reflectance with increasing wavelength is probably due to the decrease in refractive index of keratin with increasing wavelength [normal dispersion (Leertouwer et al., 2011)].

The transmitted light view shown in Fig. 2C, where the barb is very dark, suggests that throughout the barb the red pigment is highly concentrated. A cross-section of a red feather area (Fig. 3A, in this case of a Panama Amazon feather; see Fig. 6A, region 6) shows,

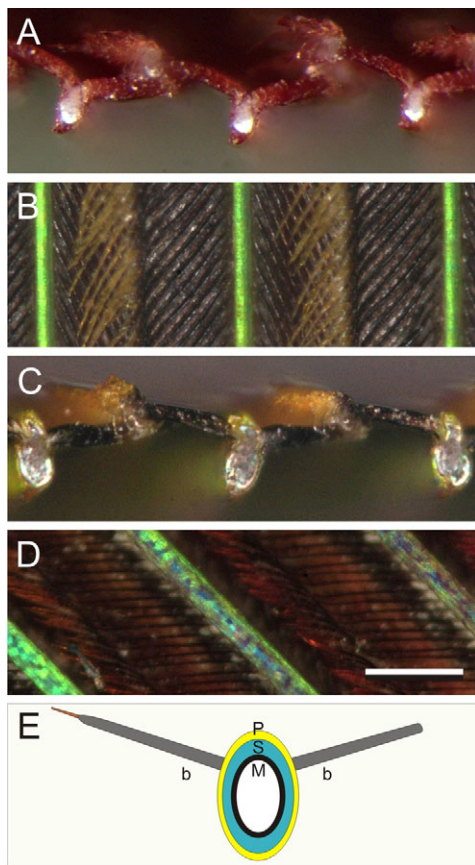


Fig. 3. Close-up views of various parts of Amazon parrot feathers. (A) A section of a feather with red pigment in both barbs and barbules (area 6 in Fig. 6A). (B) A normal view of a dark-green area (area 3 in Fig. 6C), where the barbs reflect bright green and the barbules are black because of melanin pigment; the hooklets at the distal barbules are much less pigmented and/or contain pheomelanin. (C) The same area as shown in B but perpendicularly sectioned. (D) A transition area (between areas 2 and 6 in Fig. 6A) where the barbs are filled with cells, part of which reflect green and others blue; the barbules are black or red pigmented. Scale bar (applies to A–D), 200 μ m. (E) Diagram of a cross-sectioned, structural coloured barb with barbules (b). The barb outer layer, which contains blue-absorbing, yellow pigment (P), envelopes a blue-green reflecting spongy layer (S), which is backed by black, melanin granules (M). The inner core is made up of a whitish scattering, more-or-less randomly structured material.

however, that only the outer layer of the barb contains red pigment, and that the barb's central area is filled with apparently unpigmented, distinctly whitish scattering material. The barbules, including the hooklets, are more or less homogeneously red pigmented.

Structural coloration

Generally, barbs and barbules can have quite differentiated appearances, as is for instance clear in Fig. 3B, which gives a normal view of a dark-green feather area (region 3 in Fig. 6C). The barbules are black and the hooklets at the distal barbules are brown, indicating differences in melanin pigmentation. More strikingly, the barbs are green coloured. A cross-section of the same area (Fig. 3C) also shows the black-pigmented barbules and brown hooklets, but the barb inside is again mainly whitish. Close inspection of the barb's

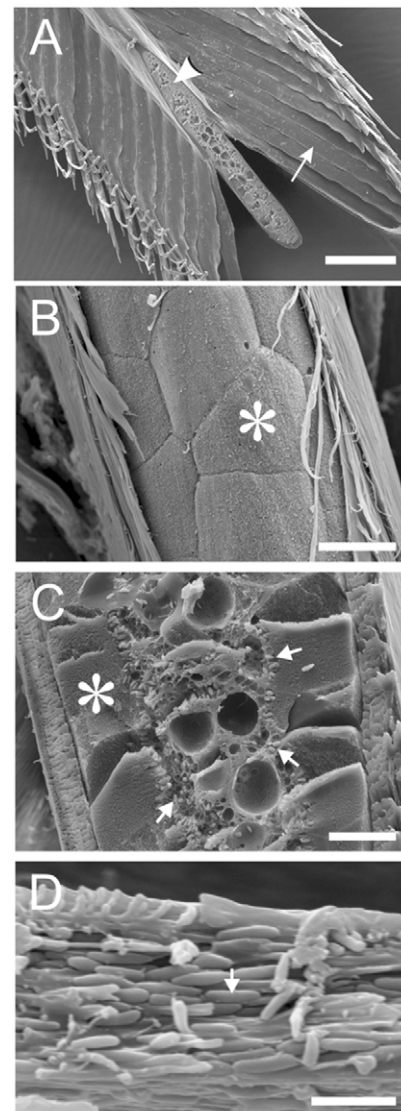


Fig. 4. Scanning electron micrographs of a green barb and black barbules of a green feather of a Panama Amazon parrot. (A) Oblique section showing the barb (arrowhead) with the attached barbules (arrow). (B) With the barb envelope removed, spongy cells (asterisk) are exposed. (C) Close-up view of a sectioned barb, showing the outer cortex with the layer of the spongy cells (asterisk), which are at the inner side lined with pigment granules (small arrows). (D) A sectioned black barbule densely packed with melanin pigment granules (arrow). Scale bars: (A) 100 μ m; (B,C) 10 μ m; (D) 2 μ m.

outer layer reveals that the material there is blue-green, yellow or greenish coloured, depending on the location. The complexity of this diverse coloration becomes clearer from a normal view of a transition area (Fig. 3D; in between regions 2 and 6 in Fig. 6A), which shows barbules that are patchily coloured blue-green and distinct green (the local barbules are black and reddish). Sections indicate that the barbules contain blue-green scattering cells bordered on the outside by a yellow-pigmented layer and on the inside by black pigment (schematically shown in Fig. 3E) [cf. fig. 2A of D'Alba et al. (D'Alba et al., 2012); see also Fig. 4]. In the green barbules (Fig. 3B), the yellow-pigmented layer is continuous, but in the patchily coloured barbules (Fig. 3D) the yellow pigmentation is discontinuous. The yellow pigment absorbs blue light on its way in as well as out of the barb, causing the green colour. When the pigment is absent, a blue-green colour remains.

To further clarify and extend the light microscopic observations, we performed scanning electron microscopy (Fig. 4). Fig. 4A shows an obliquely sectioned barb with the attached barbules of a dark-green feather area (Fig. 3B,C). Gentle removal of the cortex enveloping the barb revealed a layer of cells with a spongy fine structure (Fig. 4B; see also supplementary material Fig. S1). The spongy cells are lined by an array of granules around the central axis (Fig. 4C). These granules closely resemble the granules seen in sections of the black barbules (Fig. 4D), indicating that the granules contain melanin. The layer of these melanosomes creates an absorbing barrier between the spongy cells and the barb's central core, which consists of irregularly structured, distinctly scattering cells (Fig. 3C, Fig. 4C). The spongy cells only scatter short-wavelength, blue-green light so that in the absence of the melanosome layer long-wavelength light would reach the central cells. This would result in a background of reflected and scattered long-wavelength light, and thus in a weakened hue. In the red barbules shown in Fig. 3A no black granules are present, which makes sense because the scattering by the core cells then instead distinctly enhances the red hue.

The isolated spongy structures, exposed when the cuticular cortex was removed, featured either a blue or a blue-green colour. The difference in reflectance is clear from the spectra shown in Fig. 5A. In the case of the blue sponges, the cortex appeared to be invariably colourless, but the blue-green reflecting sponges were (virtually) always covered by a yellow-pigmented cortex (see also below).

Thin film barbules

Anatomical sections of the barbules show that they approximate thin layers, making them attractive for quantitative study of their thickness and pigmentation. Measurement of the reflectance with an MSP from a small area (20 μm square) of a red barbule yielded spectra with a valley around 500 nm (Fig. 5B), similar to the reflectance spectra measured with a reflection probe from larger areas of the intact feathers (Fig. 2D). However, a periodic oscillation was superimposed on the local reflectance spectra, immediately revealing that the barbule acts as a thin film. Similar oscillations were obtained in microspectrophotometric reflectance measurements on black and yellow barbules (Fig. 5B), apparently also due to thin film interference. From the periodicity of the oscillations the barbule thickness can be derived. Taking a barbule refractive index of 1.6 (Leertouwer et al., 2011) we derived for the thickness of the yellow, black and red barbules shown in Fig. 5B average values of approximately 1.7, 2.4 and 4.0 μm , respectively [for methods, see Stavenga et al. (Stavenga et al., 2011b)].

The reflectance spectra of the yellow and red barbules have valleys at around 450 and 500 nm, clearly indicating that the

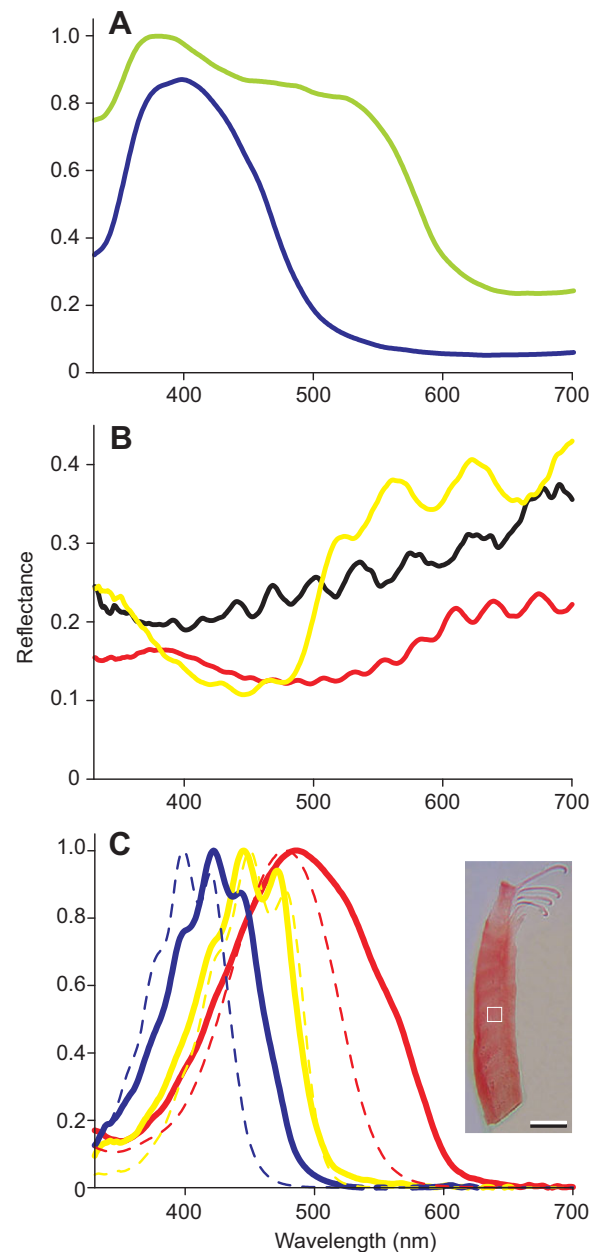


Fig. 5. Microspectrophotometry of spongy structures and single barbules, and resulting pigment absorbance spectra. (A) Local reflectance spectra of spongy structures with the cortex removed. The blue sponge had a colourless cortex, but the blue-green sponge was enveloped by a cortex with yellow pigment. (B) Reflectance spectra of a black, yellow and red barbule, measured from small areas of a Panama Amazon feather, showing oscillations due to thin film interference. (C) Normalized absorbance spectra calculated from transmittance measurements on isolated barbules in refractive index fluid. Inset: a red barbule with a 20 μm square measurement area; scale bar, 50 μm . Pale-yellow, yellow and red barbules of Panama Amazon feathers yielded the blue, yellow and red curves. For comparison, the normalized absorbance spectra of three carotenoids (e.g. Goldsmith et al., 1984; Stavenga and Wilts, 2013) are shown: galloxanthin (blue dashed), zeaxanthin (yellow dashed) and astaxanthin (red dashed).

barbules contain different psittacofulvin pigments. The shape of the absorbance spectra of the pigments can in principle be estimated from the reflectance spectra, but transmittance spectra are a more accurate source. Still, reflection losses at the barbule

surface may contaminate the transmittance spectra, and we therefore performed transmittance microspectrophotometry on barbule pieces immersed in fluids with approximately matching refractive indices (1.58–1.62). Fig. 5C shows the normalized absorbance spectra of the pigments of a pale-yellow, yellow and red barbule. The pigment densities varied among different areas of the barbules: for the (pale-)yellow and red barbules the peak absorbances were 0.10–0.15 and 0.25–0.30, respectively. Note that a density of 0.3 means a reduction of the transmittance by a factor of two, which is approximately the reduction in reflectance of the red barbule in air at 500 nm compared with the reflectance at 700 nm, where the pigment absorption is negligible (Fig. 5B,C). With a peak density of 0.3 and a thickness of 4.0 μm of the red barbule, an absorption coefficient of 0.17 μm^{-1} follows. Such a large absorption coefficient might affect the refractive index of the barbule medium (Stavenga et al., 2013). Direct refractive index measurements of the parrot barbules, however, yielded refractive index values around 1.57, very similar to those of white goose feathers (see Leertouwer et al., 2011).

Feather coloration

The psittacofulvin and melanin pigments expressed in barbs and barbules, together with the spongy barb structures, provide parrot feathers with a rich diversity of colorations (Fig. 6). Even within one and the same feather, several differently coloured areas can be distinguished, as is immediately seen on both the upper side (Fig. 6A,C) and underside (Fig. 6B,D) of two exemplary feathers of a Panama Amazon. In the black (1), yellow (5) and red (6) areas, both barbs and barbules are similarly coloured, but in the blue (2), yellow-green (4) and dark-green (3) areas the colours of barbs and barbules strongly differ (Figs 1–5, Fig. 6E). Furthermore, where the feather shown in Fig. 6A,B is on the upper side black (1) or blue

(2), it is green on the underside in both cases. The reflectance of the black area (Fig. 6F, curve 1) is obviously low at all wavelengths, indicating a high concentration of melanin pigment. The reflectance spectra of the yellow (5) and red (6) areas (Fig. 6F) resemble those shown in Fig. 2D, revealing again the presence of pigments absorbing in the blue and blue-green wavelength range (Fig. 5C). The reflectance spectrum of the blue area (Fig. 6A,E,F, area and curve 2) has the characteristic shape for structurally coloured, spongy barbs (Fig. 5A, blue curve), but the spectrum of the dark-green area (Fig. 6C,E,F, area and curve 3) strongly deviates from the reflectance spectrum of the isolated barb (Fig. 5A, green curve). Its green-peaking reflectance is due to a blue-green, broad-band reflecting spongy structure filtered by a short-wavelength-absorbing, yellow pigment (D'Alba et al., 2012; Saranathan et al., 2012). In both the blue and dark-green reflecting areas the barbules are black, because of melanin pigmentation. In the yellow-green feather area (Fig. 6A,E,F, area and spectrum 4) the barbs have a similar green colour as in the dark-green area, but the barbules are here yellow pigmented.

DISCUSSION

Amazon parrot feathers are coloured by various combinations of pigments and nanostructured components, absorbing and reflecting in restricted wavelength ranges. The absorbance spectra of the pigments of Fig. 5C confirm the interpretation that pigments selectively absorbing in the violet, blue or blue-green wavelength range prominently determine the feather reflectance. The pigments can be characterized by their peak wavelengths and bandwidth. The absorbance spectrum of the pigment of the pale-yellow feather had maxima at 422 and 443 nm and a shoulder at 400 nm; the yellow feather pigment had peaks at 445 and 471 nm and a shoulder at 423 nm. Pigments with very similar absorption spectra colour the

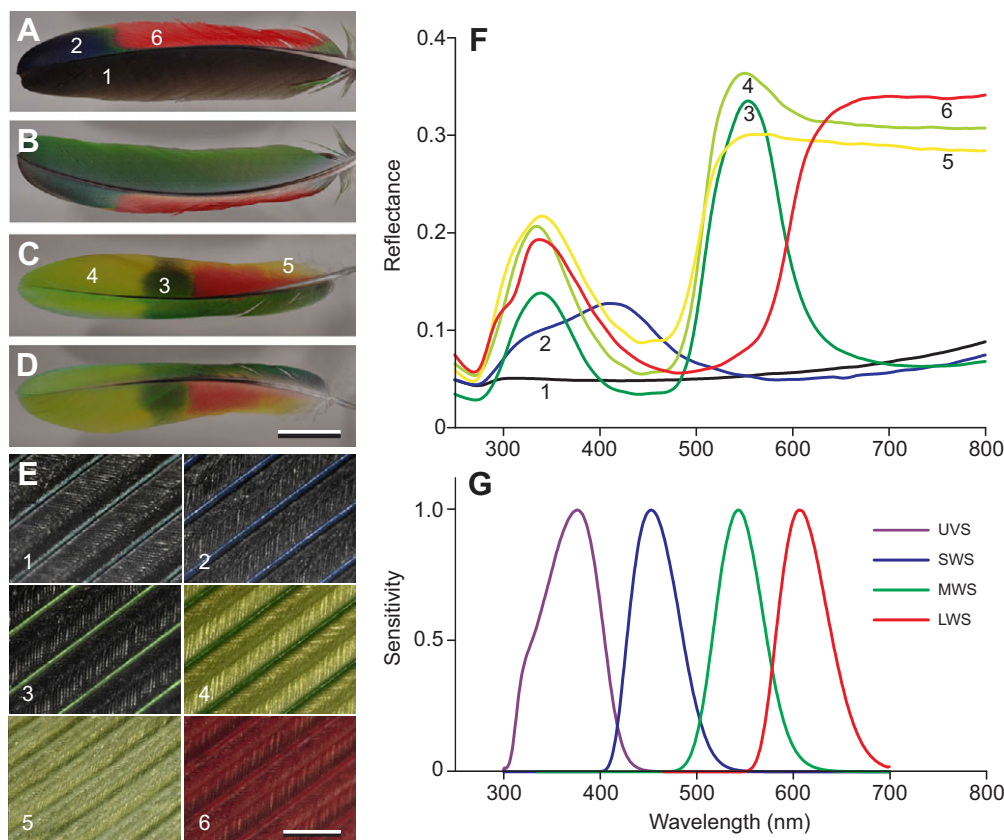


Fig. 6. Two feathers of a Panama Amazon parrot, *Amazonica ochrocephala panamensis*, and reflectance spectra. (A,C) Upper side; (B,D) underside. Scale bar (applies to A–D), 2 cm. (E) Details of the feather areas numbered 1–6 in A and C. Scale bar (applies to 1–6), 500 μm . (F) Reflectance spectra of the numbered feather areas shown in A and C, measured with a bifurcated probe. (G) Sensitivity spectra of parrot visual photoreceptors. UVS, ultraviolet sensitive; SWS, short-wavelength sensitive; MWS, middle-wavelength sensitive; LWS, long-wavelength sensitive.

feathers of passerine birds, of which lutein, zeaxanthin and β -carotene have peaks around 450 and 479 nm, with shoulders at ~425 nm. The red feather pigment of Amazon parrots has one main absorbance peak, at 486 nm (Fig. 5C), while a similar pigment of passerine feathers, astaxanthin, absorbs maximally at 478 nm (Goldsmith et al., 1984; Stavenga and Wilts, 2013). Whereas the bandwidths of the yellow pigments of Amazon and passerine feathers are rather similar (*ca.* 80 nm; Fig. 5C), the bandwidths of the two red pigments strongly differ. The full width at half maximum of the red parrot pigment is 147 nm, whilst that of astaxanthin is 96 nm (Fig. 5C). The parrot pigment thus has a much broader absorbance spectrum, extending well into the red. This will have important consequences for the feather coloration (McGraw and Nogare, 2005), and thus for its visibility.

Why the feathers of parrots are coloured by psittacofulvins and many other bird species by carotenoids remains an open question, because the parrots have ample carotenoids in their blood (McGraw and Nogare, 2004). We find that the carotenoids and psittacofulvins with peak absorbances in the blue wavelength range are spectrally very similar. Consequently, media containing these pigments will have a very similar yellow colour. Only the red parrot pigment seems to be special and able to offer a clear advantage. Its very broad absorbance spectrum may be especially suited to create a much more strikingly deep-red colour than its carotenoid counterpart, astaxanthin.

Carotenoid pigments play an important role in the eyes of both passerines and parrots (Bowmaker, 2008). Recall that bird colour vision is based on a set of four cone photoreceptor types, each with a different visual pigment, in the cone outer segment, and each with a specific oil droplet, in the cone inner segment (Hart, 2001; Cuthill, 2006; Bowmaker, 2008). Their characteristics have been studied in detail in the budgerigar (a parrot, like the Amazons). Its visual pigments, with peak wavelengths of λ_{\max} =371, 440, 499 and 566 nm, are coupled with T, C, Y and R oil droplets, respectively (Bowmaker et al., 1997; Bowmaker, 2008; Knott et al., 2012). The transparent oil droplets consist of pure lipids, but the other oil droplets contain (mainly) galloxanthin, zeaxanthin and astaxanthin (Fig. 5C) (Goldsmith et al., 1984; Stavenga and Wilts, 2013). The carotenoid pigments cause the oil droplets to act as spectral filters, placed in front of the visual pigments, thus shifting the spectral sensitivity of the cone photoreceptors towards longer wavelengths. Bird eyes have in fact another spectral filter, because the ocular media (notably the eye lens) absorb in the far UV wavelength range (Hart et al., 1998; Carvalho et al., 2011). Consequently, the spectral sensitivities of the cone photoreceptors result from the combined spectral properties of ocular media, oil droplets and visual pigments.

Calculations of the sensitivity spectra show that the ocular filtering shifts the peak wavelengths of the photoreceptors to 376, 453, 543 and 607 nm [in accordance with Hart and Vorobyev (Hart and Vorobyev, 2005), but somewhat deviating from Goldsmith and Butler (Goldsmith and Butler, 2003) (see also Berg and Bennett, 2010)]. The resulting UVS, SWS, MWS and LWS photoreceptors (Fig. 6G) are sharply tuned to restricted wavelength ranges. Comparing the spectra of Fig. 6F with those of Fig. 6G reveals some interesting correspondences. The red feather areas (Fig. 6F, curve 6) appear to particularly activate the LWS receptor; the green feathers' reflectance (Fig. 6F, curve 3) corresponds well with the MWS receptor; the reflectance of the red, green and yellow feather areas (Fig. 6F, curves 3–6) is low in the blue, where the SWS receptor is most sensitive; and in contrast, the blue feather peak reflectance (Fig. 6F, curve 2) co-localizes with the SWS receptor. All coloured feather areas have a sideband in the ultraviolet where

the UVS receptor is most sensitive. The correspondences suggest that the set of colour receptors of parrots is well tuned to discriminate the feather coloration of other parrots, particularly of conspecifics. Presumably the common green coloration of Amazon parrots (Fig. 1) functions as camouflage, and the species-specific coloration patterns serve for display and intraspecific recognition (Berg and Bennett, 2010).

ACKNOWLEDGEMENTS

Nathalie van der Vechte supplied the photograph of her pet parrot Rika (Fig. 1). Hein Leertouwer photographed the feathers shown in Fig. 2 and Fig. 6A–D.

AUTHOR CONTRIBUTIONS

D.G.S. and J.T. designed the study. All authors performed experiments and analysed data. D.G.S. wrote the manuscript.

COMPETING INTERESTS

No competing interests declared.

FUNDING

This study was financially supported by the Air Force Office of Scientific Research/European Office of Aerospace Research and Development (AFOSR/EOARD grant FA8655-08-1-3012).

REFERENCES

- Berg, M. L. and Bennett, A. T. (2010). The evolution of plumage colouration in parrots: a review. *Emu* **110**, 10–20.
- Bowmaker, J. K. (2008). Evolution of vertebrate visual pigments. *Vision Res.* **48**, 2022–2041.
- Bowmaker, J. K., Heath, L. A., Wilkie, S. E. and Hunt, D. M. (1997). Visual pigments and oil droplets from six classes of photoreceptor in the retinas of birds. *Vision Res.* **37**, 2183–2194.
- Carvalho, L. S., Knott, B., Berg, M. L., Bennett, A. T. and Hunt, D. M. (2011). Ultraviolet-sensitive vision in long-lived birds. *Proc. Biol. Sci.* **278**, 107–114.
- Cuthill, I. C. (2006). Color perception. In *Bird Coloration, Vol. 1, Mechanisms and Measurements* (ed. G. E. Hill and K. J. McGraw), pp. 3–40. Cambridge, MA: Harvard University Press.
- D'Alba, L., Kieffer, L. and Shawkey, M. D. (2012). Relative contributions of pigments and biophotonic nanostructures to natural color production: a case study in budgerigar (*Melopsittacus undulatus*) feathers. *J. Exp. Biol.* **215**, 1272–1277.
- Durrer, H. (1977). Schillerfarben der Vogelfeder als Evolutionsproblem. *Denkschr. Schweiz. Naturforsch. Ges.* **91**, 1–126.
- Goldsmith, T. H. and Butler, B. K. (2003). The roles of receptor noise and cone oil droplets in the photopic spectral sensitivity of the budgerigar, *Melopsittacus undulatus*. *J. Comp. Physiol. A* **189**, 135–142.
- Goldsmith, T. H., Collins, J. S. and Licht, S. (1984). The cone oil droplets of avian retinas. *Vision Res.* **24**, 1661–1671.
- Govardovskii, V. I., Fyhrquist, N., Reuter, T., Kuzmin, D. G. and Donner, K. (2000). In search of the visual pigment template. *Vis. Neurosci.* **17**, 509–528.
- Greenewalt, C. H., Brandt, W. and Friel, D. D. (1960). The iridescent colors of hummingbird feathers. *Proc. Am. Philos. Soc.* **104**, 249–253.
- Hart, N. S. (2001). The visual ecology of avian photoreceptors. *Prog. Retin. Eye Res.* **20**, 675–703.
- Hart, N. S. and Vorobyev, M. (2005). Modelling oil droplet absorption spectra and spectral sensitivities of bird cone photoreceptors. *J. Comp. Physiol. A* **191**, 381–392.
- Hart, N., Partridge, J. and Cuthill, I. (1998). Visual pigments, oil droplets and cone photoreceptor distribution in the European starling (*Sturnus vulgaris*). *J. Exp. Biol.* **201**, 1433–1446.
- Kinoshita, S., Yoshioka, S. and Miyazaki, J. (2008). Physics of structural colors. *Rep. Prog. Phys.* **71**, 076401.
- Knott, B., Bowmaker, J. K., Berg, M. L. and Bennett, A. T. (2012). Absorbance of retinal oil droplets of the budgerigar: sex, spatial and plumage morph-related variation. *J. Comp. Physiol. A* **198**, 43–51.
- Leertouwer, H. L., Wilts, B. D. and Stavenga, D. G. (2011). Refractive index and dispersion of butterfly scale chitin and bird feather keratin measured by interference microscopy. *Opt. Exp.* **19**, 24061–24066.
- McGraw, K. J. (2006a). Mechanics of carotenoid-based coloration. In *Bird Coloration, Vol. 1, Mechanisms and Measurements* (ed. G. E. Hill and K. J. McGraw), pp. 177–242. Cambridge, MA: Harvard University Press.
- McGraw, K. J. (2006b). Mechanics of uncommon colors: pterins, porphyrins and psittacofulvins. In *Bird Coloration, Vol. 1, Mechanisms and Measurements* (ed. G. E. Hill and K. J. McGraw), pp. 354–398. Cambridge, MA: Harvard University Press.
- McGraw, K. J. (2006c). Mechanics of melanin-based coloration. In *Bird Coloration, Vol. 1, Mechanisms and Measurements* (ed. G. E. Hill and K. J. McGraw), pp. 243–294. Cambridge, MA: Harvard University Press.
- McGraw, K. J. and Nogare, M. C. (2004). Carotenoid pigments and the selectivity of psittacofulvin-based coloration systems in parrots. *Comp. Biochem. Physiol.* **138B**, 229–233.
- McGraw, K. J. and Nogare, M. C. (2005). Distribution of unique red feather pigments in parrots. *Biol. Lett.* **1**, 38–43.

- Osorio, D. and Ham, A. D.** (2002). Spectral reflectance and directional properties of structural coloration in bird plumage. *J. Exp. Biol.* **205**, 2017-2027.
- Prum, R. O.** (2006). Anatomy, physics, and evolution of avian structural colors. In *Bird Coloration, Vol. 1, Mechanisms and Measurements* (ed. G. E. Hill and K. J. McGraw), pp. 295-353. Cambridge, MA: Harvard University Press.
- Saranathan, V., Forster, J. D., Noh, H., Liew, S. F., Mochrie, S. G., Cao, H., Dufresne, E. R. and Prum, R. O.** (2012). Structure and optical function of amorphous photonic nanostructures from avian feather barbs: a comparative small angle X-ray scattering (SAXS) analysis of 230 bird species. *J. R. Soc. Interface* **9**, 2563-2580.
- Shawkey, M. D., Estes, A. M., Siefferman, L. M. and Hill, G. E.** (2003). Nanostructure predicts intraspecific variation in ultraviolet-blue plumage colour. *Proc. Biol. Sci.* **270**, 1455-1460.
- Stavenga, D. G. and Wilts, B. D.** (2013). Oil droplets of bird eyes: microlenses acting as spectral filters. *Philos. Trans. R. Soc. B.* (in press).
- Stavenga, D. G., Leertouwer, H. L., Marshall, N. J. and Osorio, D.** (2011a). Dramatic colour changes in a bird of paradise caused by uniquely structured breast feather barbules. *Proc. Biol. Sci.* **278**, 2098-2104.
- Stavenga, D. G., Tinbergen, J., Leertouwer, H. L. and Wilts, B. D.** (2011b). Kingfisher feathers – colouration by pigments, spongy nanostructures and thin films. *J. Exp. Biol.* **214**, 3960-3967.
- Stavenga, D. G., Leertouwer, H. L. and Wilts, B. D.** (2013). Quantifying the refractive index dispersion of a pigmented biological tissue using Jamin-Lebedeff interference microscopy. *Light Sci. Appl.* **2**, e100.
- Stoddard, M. C. and Prum, R. O.** (2011). How colorful are birds? Evolution of the avian plumage color gamut. *Behav. Ecol.* **22**, 1042-1052.
- Stradi, R., Pini, E. and Celentano, G.** (2001). The chemical structure of the pigments in *Ara macao* plumage. *Comp. Biochem. Physiol.* **130B**, 57-63.
- Veronelli, M., Zerbi, G. and Stradi, R.** (1995). *In situ* resonance Raman spectra of carotenoids in bird's feathers. *J. Raman Spectrosc.* **26**, 683-692.

Supplementary Material for “Spectral tuning of Amazon parrot feather coloration by psittacofulvin pigments and spongy structures” by Tinbergen, Wilts & Stavenga

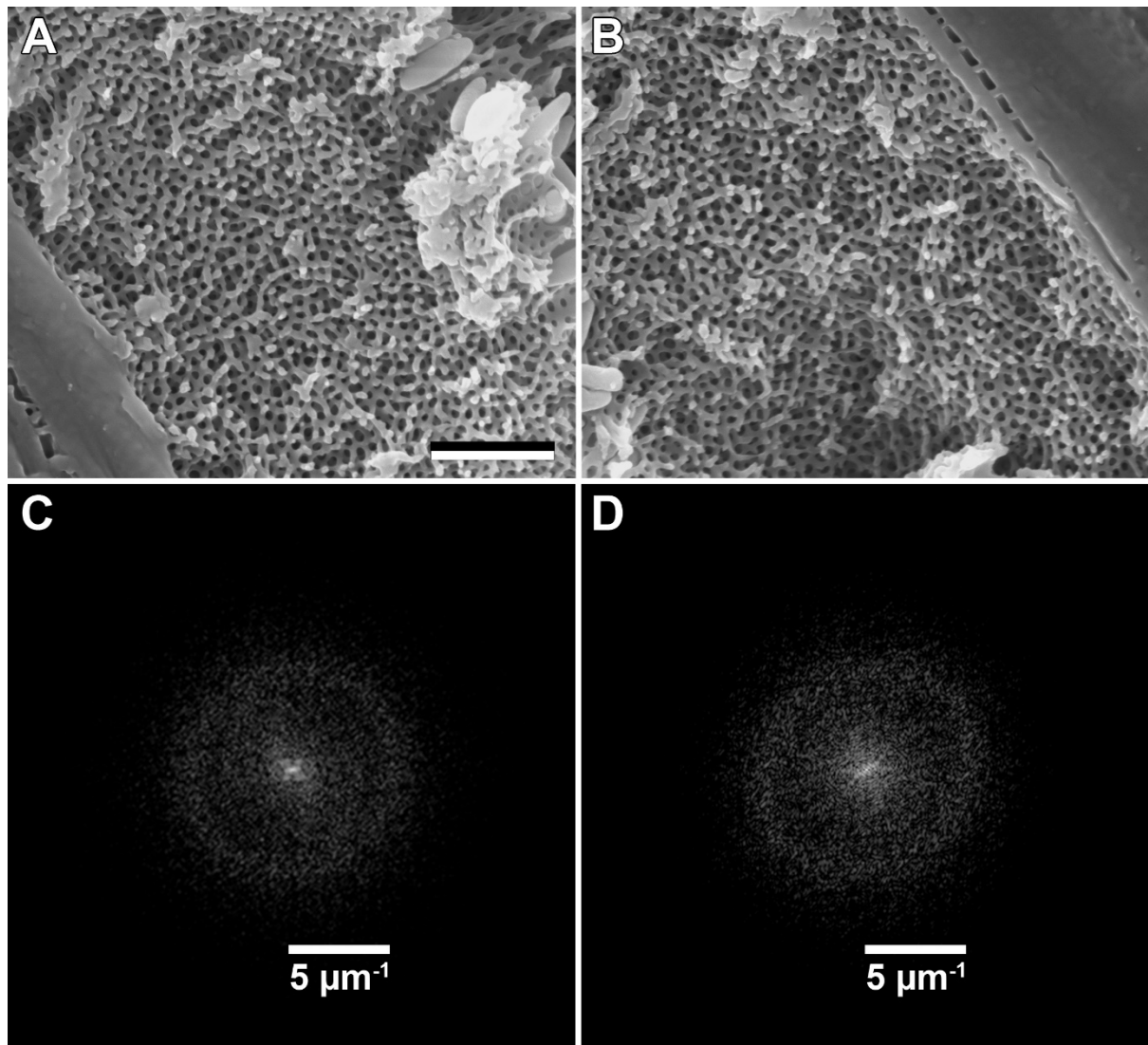


Fig. S1. Scanning electron micrographs and Fourier transforms of oblique sectioned green-colored feather barbs of a Panama amazon feather (compare Fig. 4). (A, B) Two different regions of a barb showing the inside of the spongy cells. (C, D) Power spectrum of the spongy cells of (A, B) calculated with a fast Fourier transform (FFT) using ImageJ (Schneider et al., 2012). The ring-like distribution around the centre indicates a quasi-periodic order of the spatial features (Stavenga et al., 2011; Saranathan et al., 2012). Scale bar: 2 μm (A,B). In C and D, the unit distance represents a spatial frequency of 5 μm^{-1} .

Supplementary References

Schneider, C.A., Rasband, W.S. and Eliceiri, K.W. (2012) NIH Image to ImageJ: 25 years of image analysis. *Nat. Methods* **9**, 671-675.